



## The Turbulent Graetz Problem for Direct-Contact Condensation in the Entrance Region of a Rectangular Channel

Ki Yong CHOI<sup>1)</sup> and Hee Cheon NO<sup>2)</sup>

<sup>1)</sup> Korea Atomic Energy Research Institute, 150 Dukjin-Dong, Yusong-Gu, Daejeon, 305-353, Korea

<sup>2)</sup> Korea Advanced Institute of Science and Technology, 373-1 Gusong-Dong, Yusong-Gu, Daejeon 305-701, Korea

### ABSTRACT

A new theoretical approach for direct-contact condensation heat transfer coefficients is suggested. The classical Graetz problem, which considers fully developed laminar flow through a uniform temperature duct of circular cross section, is extended to stratified condensing steam-water flows in the entrance region of a rectangular channel. The dimensionless energy equation of the turbulent water film is transformed into the Sturm-Liouville system by using separation of variables. The eddy viscosity models in near-wall and near-interface regions are incorporated to take into account the turbulence in the condensate film. Axial conduction is ignored and the interface temperature is assumed to be constant. Any instabilities or waves which may be present due to the cocurrent steam flow are neglected for simplicity. The local condensing heat transfer coefficients in the entrance region of a rectangular channel are finally obtained. The calculated heat transfer coefficients and condensing mass flow rates are compared with a database, which was constructed from the data in literature. It is found that the condensing rate of steam flow with respect to the axial coordinate is similar to the experimental data even though its value is underpredicted in the data. The local heat transfer rates are also underpredicted. It is due to the lack of accurate eddy viscosity model since the eddy viscosity model significantly affects the heat transfer rate. If a more realistic model for the eddy viscosity near interface region is available, more accurate prediction is expected.

**KEY WORDS:** condensation, direct-contact condensation, graetz problem, rectangular, horizontal, inclined, channel, entrance, developing flow, separated flow.

### INTRODUCTION

Direct-contact condensation of steam on a subcooled water is an important phenomenon in the chemical and nuclear industries. It is difficult to identify what determines the heat transfer mechanism because the transport process across the vapor-liquid interface is so complex and not fully understood yet. The phenomenon of direct-contact condensation heat transfer is characterized by the transport of heat and mass through a moving vapor-liquid interface. Due to increased turbulence in the vicinity of the vapor-liquid interface, heat transfer is enhanced. In general, the direct-contact condensation of vapor on a subcooled layer of liquid shows higher intensity of heat transfer than condensation on a cooled wall does. Stratified condensing steam-water flows are characterized with a high thermal nonequilibrium between saturated or superheated steam and subcooled water, as well as with a high slip ratio of two phases. The intensive mass, momentum and energy exchange takes place at the interface due to the condensation. In this respect, direct-contact condensation of steam on liquid layer has been an attractive subject of study for many investigators. However, most work in the past has been focused on the experimental study rather than theoretical one. ([1], [2], [3], [4], [5])

Mikielewicz and Rabe[6] provided an approximate theoretical solution of the direct-contact condensation problem, based on a simplified energy equation. They used an average liquid film velocity in the energy equation and did not consider the turbulent eddy diffusivity of heat. Mikielewicz et al.[7] suggested different physical models for direct-contact condensation in the thermal developing and developed regions. They found out that the thermal development length depends mainly on the film Reynolds number. As far as the fully developed region is concerned, it is found that nonzero value of eddy viscosity at the interface is closer to the experimental data. Choi et al. ([8],[9]) constructed a direct-contact condensation database and improved the direct-contact condensation model in the best estimate system code RELAP5/MOD3.2.

A lot of literature is available for the forced convection heat transfer in laminar flow. A excellent summary is given by Shah and London[10]. For the boundary condition of uniform wall temperature, the solutions are usually obtained in the form of an infinite series of eigenfunctions. Brown [11] solved the so-called Graetz problem in laminar flow in a circular or flat conduit numerically and obtained the first ten eigenvalues. Notter et al. [12] solved the turbulent Graetz problem numerically for the lower eigenvalues and constants. The numerical calculations incorporate new information on eddy diffusivities and are supplemented by asymptotic calculations of the higher eigenvalues and constants of the problem.

In this study, a new approach for evaluation of the direct-contact condensation heat transfer rate is suggested. It utilizes an extension of the classical turbulent Graetz problem in the entry region. It is physically based on the convective heat transfer in the turbulent liquid film at the entry region. Imagine the situation in which steam and subcooled water are stratified and cocurrently flow in a nearly horizontal channel. The entry liquid temperature is uniform, but the velocity profile is already fully developed at the point where heat transfer starts. The steam-water interface can be taken into

account the uniform wall temperature boundary condition. The mass, momentum and energy equations governing the condensate liquid flow are constructed and the direct-contact condensation heat transfer coefficients are obtained by solving the turbulent Graetz problem. The governing equations are simplified to be of dimensionless by nondimensional parameters. Any instabilities or waves which may be present due to steam flow are neglected for simplicity. The effects of the eddy viscosity in the liquid film and in the region close to the vapor-liquid interface on the heat transfer coefficients are investigated. The local heat transfer coefficients and condensing mass flow rate are calculated and compared with a database, which was constructed from the data in literature.

## MODEL DEVELOPMENT

### Eddy viscosity model

Integration of the liquid phase momentum equation gives a linear distribution of the shear stress within the liquid layer

$$\frac{\tau}{\tau_{wL}} = 1 + \frac{y}{\delta} \left( \frac{\tau_i}{\tau_{wL}} - 1 \right). \quad (1)$$

The shear stress in the turbulent liquid layer can be also presented by

$$\frac{\tau}{\tau_{wL}} = \left( 1 + \frac{\epsilon_M}{\nu_L} \right) \frac{du^+}{dy^+}, \quad (2)$$

where dimensionless variables are defined by the wall parameters as dimensionless velocity  $u^+ = u/u^*$ , dimensionless wall distance,  $y^+ = yu^*/\nu_L$ , and friction velocity  $u^* = \sqrt{(\tau_{wL}/\rho_L)}$ . The liquid phase velocity profile can be calculated by Eqs.(1) and (2),

$$u^+(y^+) = \int_0^{y^+} \frac{1 + \frac{y}{\delta} \left( \frac{\tau_i}{\tau_{wL}} - 1 \right)}{1 + \epsilon_M/\nu_L} dy^+. \quad (3)$$

In order to perform the integration of Eq.(3), an appropriate turbulence model for  $\epsilon_M(y^+)$  is required in the liquid layer. A literature survey shows that a complete turbulence model describing a condensate liquid film is not available so far. Blangetti and Schlunder[13] applied a two-layer model to the condensate film, in which a van Driest-type model for the near-wall region and a Levich-type model for the near-interface region are used. Recently, Kwon et al.[14] noticed that the dimensionless film thickness  $\delta^+$  reaches the order of 100 or above when the film Reynolds number is larger than two thousands and the two-layer model is found to be limited since the van Driest model is not applicable to the region of  $y^+$  larger than about 30. They used the van Driest-type model only when  $y^+$  is less than 30 and in the region above, the value of eddy viscosity at  $y^+ = 30$  is used until it intersects the Levich-type model. Siu-Ming Yih et al.[15] investigated the turbulent falling liquid film undergoing heating, evaporation or condensation and improved the van Driest-type model to include the effects of the interfacial shear through the variable shear stress term.

$$\epsilon_M/\nu_L = -0.5 + 0.5 \left\{ 1 + 0.64 y^{+2} \frac{\tau}{\tau_{wL}} \left[ 1 - \exp \left( \frac{-y^+}{A^+} \left( \frac{\tau}{\tau_{wL}} \right)^{\frac{1}{2}} \right) \right]^2 f^2 \right\}^{1/2}, \quad (4)$$

where  $A^+ = 25.1$ , and  $f = \exp[-1.66(1 - \tau/\tau_{wL})]$  is a damping factor. Therefore, the van Driest-type model seems to be a promising one in the near-wall region.

Ueda et al.[16] investigated the eddy diffusivity near the free surface of open channel flow and suggested a free surface eddy viscosity model based on the experimental data

$$\epsilon_M/\nu_L = \kappa Y_s^+ (1 - Y_s^+/\delta^+) \{ 1 - \exp(-Y_s^+/30.4) \}^2, \quad (5)$$

where  $\kappa$  is the von Karman constant, 0.40 and  $Y_s^+$  is dimensionless distance from the interface defined by  $Y_s^+ = \delta^+ - y^+$ .

In this study, Eq.(4) and Eq.(5) are used as a turbulence model for near-wall and near-interface region, respectively. The boundary between the near-wall and near-interface region is obtained by the intersection between two equations. Once the shear stress distribution and dimensionless film thickness are given, which will be described in the following section, the velocity profile can be computed from Eq.(3).

### Momentum conservation

A physical situation considered in this study is shown in Fig.1. A steam/water stratified flow is observed in a horizontal or a nearly inclined channel. The liquid film is subcooled and the channel walls surrounding the channel are adiabatically insulated. The saturated steam flows over the liquid film cocurrently and direct-contact condensation of the steam occurs. A liquid film having a mass flow rate of  $m_{fin}$  and temperature of  $T_e$  is injected at the entrance region and the steam of a mass flow rate of  $m_{gin}$  and temperature of  $T_g$  is cocurrently injected at the same entrance as shown in Fig.1.

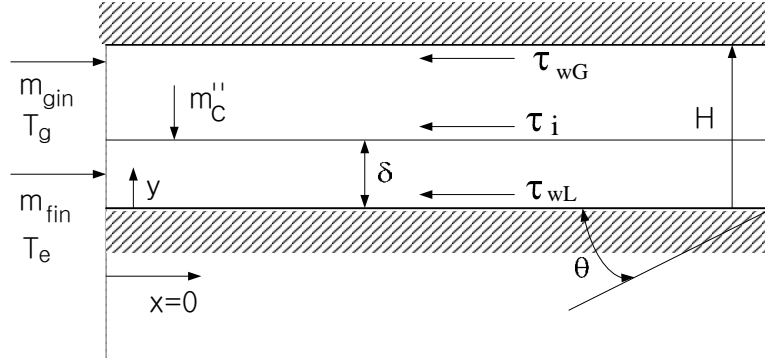


Figure 1 A physical situation for a steam/water cocurrent stratified flow

A one-dimensional momentum balance in the gas and the liquid phases is given by

$$-A_L\left(\frac{dP}{dx}\right) - \tau_{wL}P_L + \tau_iP_i + \rho_L A_L g \sin \theta = 0, \quad (6)$$

and

$$-A_G\left(\frac{dP}{dx}\right) - \tau_{wG}P_G - \tau_iP_i + \rho_G A_G g \sin \theta = 0, \quad (7)$$

where  $(dP/dx)$  is the pressure gradient,  $A$  is the phase cross-sectional area,  $\rho$  is the density,  $P$  is the perimeter over which the stress acts,  $\tau$  is the shear stress,  $g$  is the acceleration due to the gravity and  $\theta$  is the downward angle between the channel and the horizontal; subscript G and L are for gas and liquid, respectively, i for interfacial and W for the wall. In the above equation, the wall and interfacial stresses  $\tau_{wL}$ ,  $\tau_{wG}$ , and  $\tau_i$  are evaluated by  $\tau_{wL} = \frac{1}{2}f_L\rho_L u_L^2$ ,  $\tau_{wG} = \frac{1}{2}f_G\rho_G u_G^2$ ,  $\tau_i = \frac{1}{2}f_i\rho_G u_G^2$ , respectively. The friction factors,  $f_L$ ,  $f_G$ , and  $f_i$  are the same functions of the liquid and gas Reynolds numbers as in single phase flow. In the stratified flow, the gas friction factor,  $f_G$  can be assumed as in single phase flow by

$$f_G = 0.079Re_G^{-0.25}. \quad (8)$$

Hanratty and Andritsos [17] suggested a correlation for the interfacial friction factor as follows:

$$\frac{f_i}{f_G} = 1 \quad \text{for } j_{gs} < 1.5, \quad (9)$$

$$\frac{f_i}{f_G} = 1 + 0.75\left(\frac{j_{gs}}{1.5} - 1\right) \quad \text{for } j_{gs} > 1.5, \quad (10)$$

where  $j_{gs}$  is the gas superficial velocity. For an assumed liquid film thickness, the total pressure gradient  $(dP/dx)$  can be calculated from Eq.(7) with Eqs. (8), (9), (10), and the corresponding geometrical parameters. Then, the liquid phase wall shear stress,  $\tau_{wL}$  is obtained from Eq.(6) with the obtained total pressure gradient  $(dP/dx)$ . From the obtained wall shear stress,  $\tau_{wL}$ , the shear stress and eddy viscosity profiles are calculated. Finally the velocity profile is obtained by integration in the previous section. Then, condensate mass flow rate is obtained by to check mass conservation.

$$m_{fin} = \mu_L \int_0^{\delta^+} u^+ dy^+, \quad (11)$$

### Energy conservation

Once the velocity profile is known, the energy equation with the condensate film should be solved

$$u \frac{\partial T}{\partial x} = \frac{\partial}{\partial y}[(\alpha + \epsilon_H) \frac{\partial T}{\partial y}], \quad (12)$$

where  $\alpha$  and  $\epsilon_H$  are momentum and turbulent eddy diffusivity of heat, respectively. By introducing the following dimensionless quantities,  $\theta = \frac{T_g - T}{T_g - T_e}$ ,  $y^* = y/\delta$ ,  $x^* = \frac{x/\delta}{RePr}$ ,  $Re = u_{avg}\delta/\nu_L$ ,  $Pr = \nu_L/\alpha$ . into Eq.(12) the energy equation

can be cast into the following form:

$$u^+ \frac{u^*}{u_{avg}} \frac{\partial \theta}{\partial x^*} = \frac{\partial}{\partial y} [(1 + \epsilon_H/\alpha) \frac{\partial \theta}{\partial y^*}], \quad (13)$$

with the boundary conditions  $\frac{d\theta}{dy}(x, y=0) = 0$ ,  $\theta(x, y=\delta) = 0$ ,  $\theta(x=0, y) = 1$ , where the interface temperature,  $T_g$  and the inlet liquid temperature  $T_e$  are assumed to be constant. By using the separation of variables, Eq.(13) can be rewritten by

$$\frac{\partial}{\partial y^*} [P(y^*) Y'] + \lambda^2 R(y^*) Y = 0, \quad (14)$$

$$X' + \frac{u_{avg}}{u^*} \lambda^2 X = 0, \quad (15)$$

with the boundary conditions  $Y(1) = 0$ ,  $Y'(0) = 0$ , and  $X(0)Y(y^*) = 1$ , where  $\lambda$  is the eigenvalue of the Eq.(14) and

$$P(y^*) = 1 + \epsilon_H/\alpha, \quad (16)$$

$$R(y^*) = u^+(y^*). \quad (17)$$

Equation (16) can be represented using the turbulent Prandtl number

$$P(y^*) = 1 + \frac{Pr}{Pr_t} \epsilon_M/\nu_L, \quad (18)$$

where the turbulent Prandtl number  $Pr_t$  is assumed to be unit.

The energy equation is reduced to a classical Sturm-Liouville system with a complete set of eigenfunctions orthogonal with respect to a weighting function,  $R(y^*)$ . (Boyce et al. [18]) The solution of the above equation can be written as :

$$\theta(x^*, y^*) = \sum_{n=1}^{\infty} C_n Y_n(y^*) \exp(-\frac{u_{avg}}{u^*} \lambda_n^2 x^*), \quad (19)$$

where  $\lambda_n$  is an eigenvalue and  $Y_n(y^*)$  is the corresponding eigenfunction. The  $C_n$  are constants and determined by the boundary condition  $X(0)Y(y^*) = 1$ , i.e.,

$$\sum_{n=1}^{\infty} C_n Y_n = 1. \quad (20)$$

Numerically, the coefficients,  $C_n$  is determined by considering finite N eigenmodes ( $\lambda, Y_n(y^*)$ ) adequate for a converged solution. The method of weighted residuals is used. Applying the boundary condition at the entrance, multiplying Eq.(20) by  $Y_m$  and integrating over  $0 \leq y^* \leq 1$ , we obtain

$$\sum_{n=1}^N C_n \int_0^1 Y_m Y_n dy = \int_0^1 Y_m dy \quad \text{for } m = 1, 2, \dots, N. \quad (21)$$

Solving the above set of N simultaneous equations, the coefficient  $C_n$  are determined.

The superscripts dropped for the convenience, Eq.(14) can be reduced to the system of the first order differential equations as follows:

$$\frac{\partial Y_1}{\partial y} = Y_2, \quad (22)$$

$$\frac{\partial Y_2}{\partial y} = -\frac{P'}{P} Y_2 - \frac{R}{P} Y_1 Y_3, \quad (23)$$

$$\frac{\partial Y_3}{\partial y} = 0, \quad (24)$$

with the boundary conditions

$$Y_1(0) = 1, Y_1(1) = 0, \quad (25)$$

$$Y_2(0) = 0, \quad (26)$$

$$Y_3 = \lambda^2, \quad (27)$$

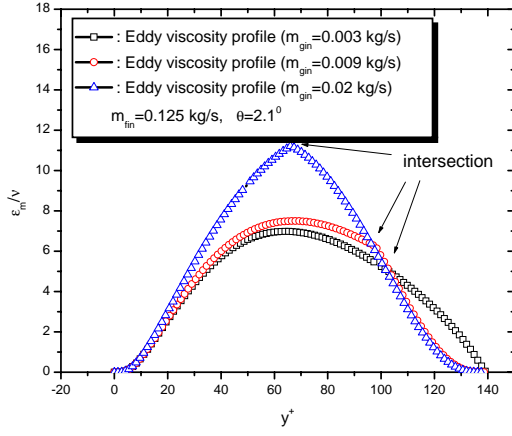


Figure 2 A calculated eddy viscosity profile

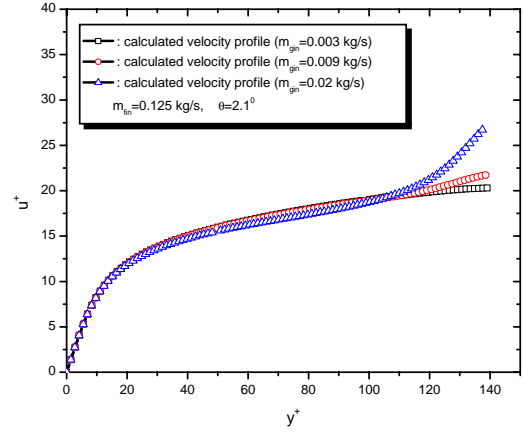


Figure 3 A calculated velocity profile

where  $Y_1 = Y$ ,  $Y_2 = dY/dy$ , and  $Y_3 = \lambda^2$ . The eigenvalues and the corresponding eigenfunctions are calculated as follows: First, the eigenvalue  $\lambda^2$  is initially guessed to be zero and the system of order differential equations are solved by the Runge-Kutta method from  $y = 0$  to  $y = 1$ . When the calculation finishes at the final value of  $y = 1$ , the value of the  $Y_1(1)$  is checked whether it converges to zero. If not, the initial guess of the eigenvalue  $\lambda^2$  is increased until the convergence reached. Once the principal eigenvalue  $\lambda_1^2$  is found, the initial guessing is further increased to find other higher order eigenvalues, since all eigenvalues in the Sturm-Liouville system are real positive and can be ordered so that  $\lambda_1 < \lambda_2 < \dots$ , and  $\lambda_n \rightarrow \infty$  as  $n \rightarrow \infty$ . In this study, the first six eigenvalues are obtained with double precision accuracy. The present solution algorithm is confirmed since it successfully reproduces the eigenvalues  $\lambda_n^2$ , eigenfunctions  $Y_n$ , coefficients,  $C_n$  which are known in literature for laminar convection flow.

The dimensionless bulk temperature,  $\theta_m$  and the local Nusselt number  $Nu(x)$  are then determined as

$$\theta_m = \frac{T_g - T_m}{T_g - T_e} = \frac{1}{\delta u_{avg}} \int_0^\delta u \theta dy = \frac{u^*}{u_{avg}} \int_0^1 R(y) \theta dy. \quad (28)$$

If Eq.(19) is plugged into the above equation,

$$\theta_m = \frac{u^*}{u_{avg}} \sum C_n \exp\left(-\frac{u_{avg}}{u^*} \lambda_n^2 x\right) \int R(y) Y_n dy. \quad (29)$$

$$Nu(x) = \frac{1}{\theta_m} \frac{d\theta}{dy} \Big|_{y=1} = \frac{\sum C_n Y_n'(1) \exp\left(-\frac{u_{avg}}{u^*} \lambda_n^2 x\right)}{\theta_m} = \frac{2 \sum G_n \exp\left(-\frac{u_{avg}}{u^*} \lambda_n^2 x\right)}{\theta_m}, \quad (30)$$

where  $G_n = -0.5 C_n Y_n'(1)$ . Therefore, the local heat transfer coefficient is obtained by  $h(x) = \frac{k_L}{\delta} Nu(x)$ , where  $k_L$  is thermal conductivity of the liquid film.

## RESULTS AND RECOMMENDATIONS

### Eddy viscosity and velocity profiles

Figure 2 shows the eddy viscosity profile across the condensate liquid film in an inclined channel of  $2.1^\circ$  at the inlet liquid and steam flow rates of  $m_{fin} = 0.125 \text{ kg/s}$ . The steam flow rate increases from  $m_{gin} = 0.003 \text{ kg/s}$  to  $m_{gin} = 0.02 \text{ kg/s}$ . As can be seen in the figure, the effect of steam flow rate on the eddy viscosity profile is noticeable. As the steam flow rates increases, the eddy viscosity in the center region becomes greater. Figure 3 shows the calculated velocity profile within the condensate liquid film. The effect of steam flow rates is also plotted in the same figure. As the steam velocity increases, the interface velocity becomes large due to the increased interfacial shear. However, the velocity inside the condensate liquid film is not so affected by the increased steam flow rate. The calculated liquid film thickness is plotted in figure 4 against the database. (Choi. et al. [9]) As can be seen in the figure, the liquid film thickness is within the error boundary of 20%.

### Eigenvalues and eigenfunctions

Table 1 shows the first six eigenvalues which are calculated for the case of  $m_{fin} = 0.125 \text{ kg/s}$ ,  $m_{gin} = 0.012 \text{ kg/s}$ , and  $\theta = 5.0^\circ$ . Using the obtained eigenvalues,  $\lambda_n^2$  and the coefficients,  $C_n$  and  $G_n$ , the temperature profile, dimensionless temperature and heat transfer coefficient can be calculated.

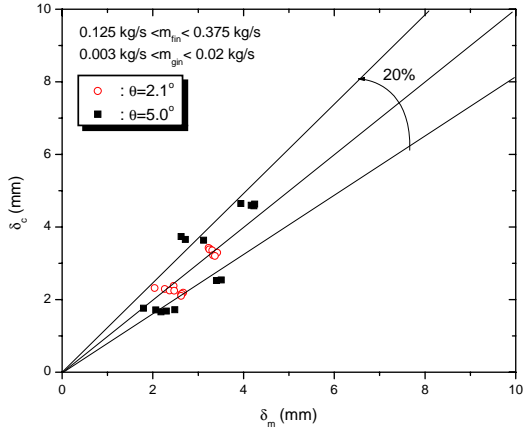


Figure 4 The comparison of the calculated liquid film thickness with the data

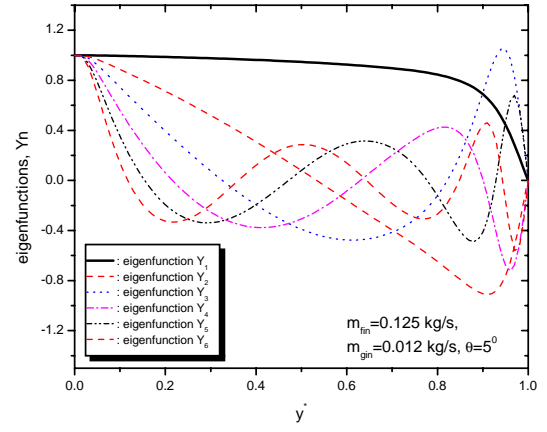


Figure 5 The calculated eigenfunctions

Table 1 The calculated first six eigenvalues

$n$	$\lambda_n^2$	$C_n$	$G_n$
1	0.710316	1.111716	5.411520
2	16.659223	-0.223546	2.146177
3	39.313235	0.226082	3.604869
4	71.846764	-0.205941	2.993877
5	112.998222	0.210659	3.598921
6	164.183220	-0.151661	2.622010

Figure 5 shows the behavior of the first six eigenfunctions for the same case. The eigenfunctions satisfy the orthogonality relations

$$\int_0^1 Y_n(y)Y_m(y)R(y)dy = 0, \quad \text{for } m \neq n. \quad (31)$$

### Temperature profile

Figure 6 indicates the temperature profile within the condensate film for various axial positions,  $x = 0$ . It can be seen from the figure, temperature starts to develop at the entrance position,  $x = 0$ . Figure 7 shows the dimensionless average liquid film temperature,  $\theta_m$  with respect to axial location. No significant difference in  $\theta_m$  is not observed even though the initial gas flow rates increase.

### Local steam flow rates and heat transfer coefficients

If steam temperature is assumed to be constant, differential macroscopic energy balance in a rectangular channel is written by

$$dq = h_x b [T_g - T(x)] dx = d[m_f(x) i_f(x)] = -i_{fg} d[m_g(x)], \quad (32)$$

where the liquid enthalpy is defined by  $i_f(x) = C_{pf} T(x)$ . Then Eq.(32) is expressed by

$$h_x b [T_g - T(x)] dx = C_{pf} m_f(x) dT(x) + C_{pf} T(x) dm_f(x). \quad (33)$$

Integration of Eq.(32) from  $x = 0$  to  $x$  gives

$$C_{pf} m_f(x) T(x) - C_{pf} m_{f,e} T_e = i_{fg} [m_{g,e} - m_g(x)]. \quad (34)$$

The relationship between  $m_g(x)$  and  $m_f(x)$  can be obtained from the mass balance as follows:

$$m_f(x) - m_{f,e} = m_{g,e} - m_g(x). \quad (35)$$

Substitution of Eq.(35) into Eq.(34) gives

$$m_f(x) [C_{pf} T(x) - i_{fg}] = m_{f,e} [C_{pf} T_e - i_{fg}]. \quad (36)$$

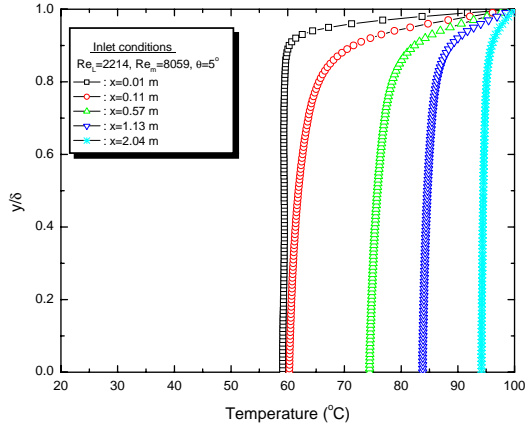


Figure 6 The calculated temperature profile

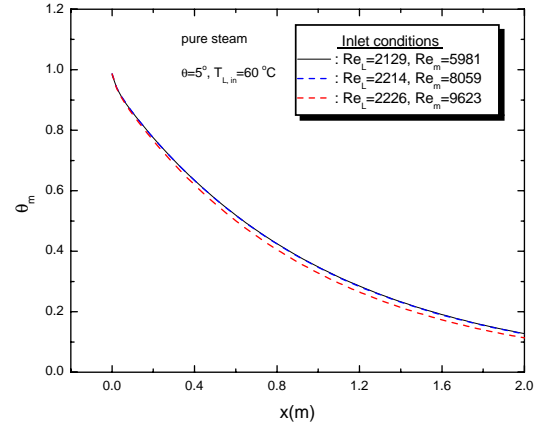


Figure 7 Axial variation of the calculated dimensionless average temperature

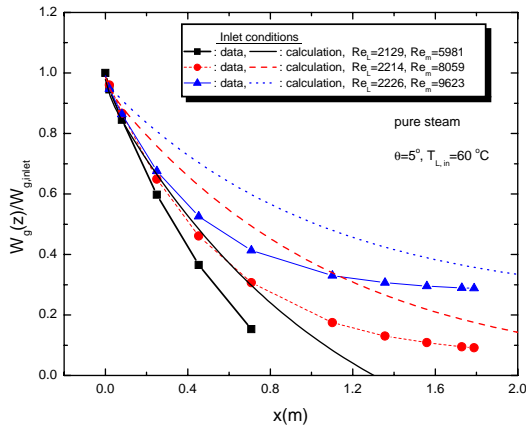


Figure 8 Axial variation of the calculated steam flow rate

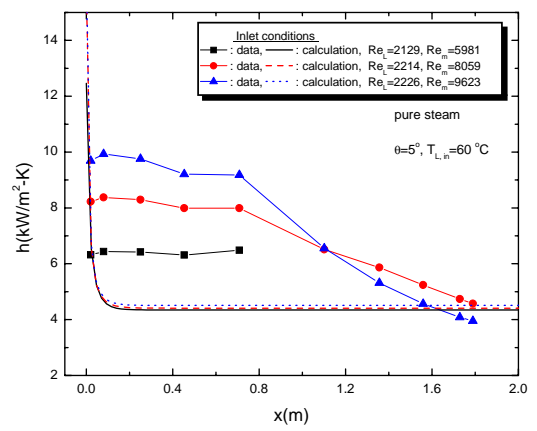


Figure 9 Axial variation of the heat transfer coefficients

Arrangement of Eq.(36) gives

$$m_f(x) = \frac{m_{f,e}(C_{pf}T_e - i_{fg})}{C_{pf}T(x) - i_{fg}}. \quad (37)$$

The local steam mass flow rate can be obtained from Eqs.(35) and (37). The experimental work by the authors is described in detail elsewhere ([8],[9]). The test section is a nearly inclined rectangular channel, 1.8m long, 0.12m wide, and 0.04m high. Steam at atmospheric pressure is supplied from a boiler through a separator and a throttling valve to ensure a dry saturated state at the entrance to the test section. Demineralized water is introduced to the test section. The theoretical steam flow rate can be computed from the following equation, once  $\theta_m$  is obtained.

$$\theta_m = \frac{T_g - T_m}{T_g - T_e}. \quad (38)$$

Figure 8 shows a comparison of the theoretical steam mass flow rates and the experimental values. Lower condensing rates than the experimental data are predicted.

The calculated local heat transfer coefficient is plotted in figure 9 against the experimental data. It can be seen from the figure that the thermal development length is very short about 0.1m from the entrance. The calculated heat transfer coefficients is greatly under-estimated compared with the data. It is probably due to the incorrect eddy viscosity profile near the interface region. If higher value of eddy viscosity is tried, much large heat transfer coefficients are obtained. However, we did not succeed to quantify the effects of the eddy viscosity on the heat transfer coefficients at the moment. It is expected that much improved results can be obtained if more detailed eddy viscosity profile is available.

## CONCLUSIONS

The present work theoretically investigates the direct-contact condensation of steam on horizontally stratified sub-

cooled water in a rectangular channel. As a new approach, the turbulent Graetz problem is extended with a uniform wall temperature boundary condition for the application of the direct-contact condensation. The van Driest-type eddy viscosity model is used in the near-wall region and Ueda's eddy diffusivity model near the free surface of open channel flow is used for the near-interface region. Based on the eddy viscosity model, the velocity profile in the condensate film and the condensate film thickness are obtained. Axial conduction is ignored and the interface temperature is assumed to be constant in the energy conservation. The local steam flow rates and the local heat transfer coefficients are computed. It is found that the condensing rates of the steam flow is under-estimated from that of the experimental data.

The local heat transfer rates are under-estimated due to the lack of accurate eddy viscosity model near the interface region. Since, the eddy viscosity model significantly affects the heat transfer rate, further investigation on the eddy viscosity near the vapor-liquid interface is required for a more accurate prediction. Even though, the present model does not reproduce the experimental data, its approach can be considered to be one method to model the direct-contact condensation in stratified two-phase flow. It is expected that much improved results can be obtained if more detailed eddy viscosity profile is available.

## References

- [1] A. Segev et al. (1981), "Experimental study of countercurrent steam condensation," *ASME, J. Heat Transfer*, **103**, pp307-311.
- [2] S. G. Bankoff and H. J. Kim (1983), "Local condensation rates in nearly horizontal stratified countercurrent flow of steam and cold water," *AIChE Symp. Ser.* **79**, pp209-223.
- [3] I. S. Lim et al. (1984), "Condensation measurement of horizontal cocurrent steam/water flow," *ASME J. Heat Transfer*, **106**, pp425-432.
- [4] H. J. Kim, S. C. Lee and S. G. Bankoff (1985), "Heat transfer and interfacial drag in countercurrent steam water stratified flow," *Int. J. Multiphase Flow*, **11**, pp593-606.
- [5] H. Ruile (1995), "Heat transfer by direct contact condensation in stratified two phase flow at high system pressure," *Proc. of the 1st Int. Symposium on Two-Phase Flow Modelling and Experimentation, Rome, Italy*, **1**, pp269-276
- [6] J. Mikieliewicz and A.M.A. Rageb (1995), "Simple theoretical approach to direct-contact condensation on subcooled liquid film," *Int. J. Heat Mass Transfer*, **38**, pp-557-562.
- [7] J. Mikieliewicz et al. (1997), "A theoretical and experimental investigation of direct-contact condensation on a liquid layer," *Exp. Thermal and Fluid Sci.*, **15**, pp221-227.
- [8] K.Y. Choi et al. (1998), "Assessment and improvement of condensation models in RELAP5/MOD3.2," *Nuclear Technology*, **124**, pp103-117.
- [9] K.Y. Choi et al. (2002), "Direct-contact condensation heat transfer model in RELAP5/MOD3.2 with/without non-condensable gases for horizontally stratified flow," *Nuclear Engineering and Design*, **211**, pp139-151.
- [10] R.K. Shah and A. L. London (1978), "Laminar Flow Forced Convection in Ducts," *Advances in Heat Transfer*, **15**.
- [11] G. M. Brown (1960), "Heat or mass transfer in a fluid in laminar flow in a circular or flat conduit," *AIChE J.*, **6**, pp179-183.
- [12] R.H. Notter and C.A. Sleicher (1972), "A solution to the turbulent Graetz problem-III Fully developed and entry region heat transfer rates," *Chem. Eng. Sci.*, **27**, pp2073-2093.
- [13] F. Blangetti and E.U.Schlunder (1978), "Local heat transfer coefficients on condensation in a vertical tubes," *Proc. of the 6th Int. Heat Transfer Conf.*, **2**, pp437-442.
- [14] J.T. Kwon et al. (2001), "A modeling of in-tube condensation heat transfer for a turbulent annular film flow with liquid entrainment," *Int. J. Multiphase Flow*, **27**, pp911-928.
- [15] Siu-Ming Yih and Jung-Liang Liu (1983), "Prediction of heat transfer in turbulent falling liquid films with or without interfacial shear," *AIChE J.*, **29**, pp903-909.
- [16] Hiromasa Ueda et al. (1977), "Eddy diffusivity near the free surface of open channel flow," *Int. J. Heat Mass Transfer*, **20**, pp1127-1136.
- [17] T. J. Hanratty and N. Andritsos (1984), "Effect of pipe diameter on stratified flow in horizontal pipes," *Univ. of Illinois, Urbana III*.
- [18] W.E. Boyce and R.C. DiPrima (1977), "Elementary differential equations and boundary value problems," John Wiley and Sons, Third Edition.